

Report No.: SIR-05-007  
Revision No.: 0  
Project No.: CCNP-04Q  
File No.: CCNP-04Q-401  
January 2005

**Minimum Chromium Content In  
Nickel-Alloy Weld Overlays to  
Mitigate PWSCC**

*Prepared for:*

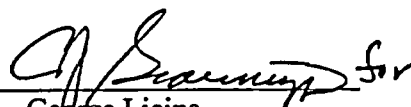
Welding Services Inc.  
Contract or PO Number: 32032

*Prepared by:*

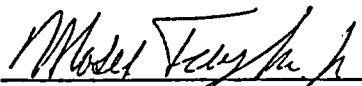
Structural Integrity Associates, Inc.  
San Jose, California

*Prepared by:*   
Barry M. Gordon, P.E.

Date: 1/14/05

*Reviewed by:*   
George Licina

Date: 1/18/05

*Approved by:*   
Moses Taylor, P.E.

Date: 1/18/05

**REVISION CONTROL SHEET**

Document Number: SIR-05-007

Title: Minimum Chromium Content In Nickel-Alloy Weld Overlays to Mitigate PWSCC

Client: Welding Services Inc.

SI Project Number: CCNP-040

Section	Pages	Revision	Date	Comments
1.0	1-1 – 1-8	0	1/13/05	Initial Issue
2.0	2-1 – 2-8			
3.0	3-1 – 3-4			
4.0	4-1 – 4-1			

Table of Contents

<u>Section</u>	<u>Page</u>
<b>1.0 EFFECT OF CHROMIUM CONTENT ON NICKEL-BASE ALLOY PWSCC RESISTANCE.....</b>	<b>1-1</b>
1.1 Introduction.....	1-1
1.2 Chromium Content “Threshold” for PWSCC Resistance .....	1-1
1.3 Discussion.....	1-3
1.4 Conclusion .....	1-4
<b>2.0 CHROMIUM MEASUREMENT TECHNIQUE - X-RAY FLUORESCENCE.....</b>	<b>2-1</b>
2.1 Introduction.....	2-1
2.2 Background.....	2-1
2.3 Sample Analysis Techniques .....	2-2
2.4 Methodology.....	2-2
2.5 Analytical Aspects .....	2-3
<b>3.0 CHROMIUM CONTENT MEASUREMENT LOCATIONS.....</b>	<b>3-1</b>
3.1 Introduction.....	3-1
3.2 Measurement Locations.....	3-1
<b>4.0 REFERENCES.....</b>	<b>4-1</b>

## List of Tables

<u>Table</u>	<u>Page</u>
Table 1-1 Compositions of Nickel-base Alloys and Weld Metals .....	1-5
Table 2-1 Examples of Precision of XRF Analyzer Measurements [12] .....	2-5
Table 3-1 XRF Measurement Locations Priorities .....	3-3

## List of Figures

<u>Figure</u>	<u>Page</u>
Figure 1-1. Effect of Chromium Content on the Stress Corrosion Cracking Resistance of Solution Annealed Ni-Cr-Fe Alloys [7].....	1-6
Figure 1-2. Oxide Film Developed on Alloy 600 (a) and Alloy 690 (b) [8] .....	1-6
Figure 1-3. Composition of Ni, Cr and Fe as a Function of the Distance from the Metal-Oxide Interface on Alloy 600 (a) and Alloy 690 (b) .....	1-7
Figure 1-4. Sketch of the Oxide Film Developed on Alloy 600 and Consequences on the Underlying Metal [8].....	1-7
Figure 1-5. Sketch of the Depletion in Chromium under the Oxide Scale Associated with Enrichment in Oxygen at a Triple Grain Boundary [8] .....	1-8
Figure 2-1. XRF Excitation Model [11] .....	2-6
Figure 2-2. Metal Sample Fluorescence [11].....	2-6
Figure 2-3. Schematic of XRF Instrument [11].....	2-7
Figure 2-4. Correlation Plot for Cr and Mo in Various Fe, Co and Ni Alloys [12].....	2-8
Figure 3-1. Sketch of XRF Inspection Locations .....	3-4

## **1.0 EFFECT OF CHROMIUM CONTENT ON NICKEL-BASE ALLOY PWSCC RESISTANCE**

### **1.1 Introduction**

The only well established correlation between primary water stress corrosion cracking (PWSCC) propensities and nickel-based alloys and weld metal composition is the chromium content of the alloy [1]. However, there have been very few systematic studies to determine the minimum chromium content for PWSCC mitigation in either wrought materials or weld metals. Most studies have involved a straightforward comparison of Alloy 600 with 14-17% chromium and Alloy 690 with 28-31% chromium with no testing of custom nickel-chromium-iron alloys whose chromium content falls in between these two alloys. This absence creates a chromium compositional gap between the susceptible Alloy 600/182/82 and very resistant Alloy 690/152/52.

Table 1-1 presents the nominal chemical compositions of nickel-base weld metals plus reference wrought Alloys 690 and 600 for each weld metal, i.e., Alloys 52, 152 and 72 for Alloy 690 and Alloys 82, 182, and 132 for Alloy 600 [2-5]. Based on chromium content, it would be anticipated that weld metals Alloys 52, 152 and 72 would be the most PWSCC resistant and this hypothesis has been verified by experiment.

### **1.2 Chromium Content “Threshold” for PWSCC Resistance**

To determine the “threshold” chromium content of a nickel-base weld metal to mitigate PWSCC, it is necessary to review the limited test results obtained in PWR environments and also examine the results from tests on wrought nickel alloys. Note that there is also some information obtained in oxygenated environments. However, this data is also largely characterized by Alloy 600 versus Alloy 690 investigations.

The PWSCC resistance of nickel-based weld metals with various chromium contents ranging from approximately 15% to 30% chromium has been evaluated [1,6]. Testing was performed on

U-bend specimens exposed to impurity doped steam and primary water. Alloy 182, with approximately 14.5% chromium, was the most susceptible to PWSCC while Alloy 82 with 18–20% chromium took three or four times longer to initiate PWSCC. For example, PWSCC appeared in one of the Alloy 182 specimens at the first test interruption after 500 hours of exposure and the second specimen cracked after 1,500 hours. The first Alloy 82 specimen cracked after 2,000 hours and all were cracked at 6,500 hours. For chromium contents between 21 and 22%, no PWSCC initiation was observed for tests lasting between 18,000 and 27,000 hours. This was also the case for Alloys 52 and 152 that have approximately 30% chromium. These results indicated that weld metals with 30% chromium were very resistant to PWSCC, with a “threshold” for PWSCC resistance being between 22 and 30% chromium.

The above PWSCC behavior is consistent, i.e., higher chromium content provides more PWSCC resistance, with the test results on solution annealed wrought Ni-Cr-Fe base alloys [1,7]. Constant load tests were used to evaluate the effect of chromium content on the PWSCC susceptibility of wrought Ni-Cr-Fe alloys in 680°F (360°C) water. The constant load specimens were loaded at an applied stress 2.4 times the 0.2% proof stress. Figure 1-1 clearly demonstrates that the PWSCC initiation susceptibility decreased as the chromium content increased from approximately 1% to over 15% [1,7]. However, this study did not evaluate higher chromium alloys (e.g., 18-22% Cr) and even suggests that Alloy 600 with 17% chromium would be PWSCC resistant.

To possibly identify a chromium content “threshold” for PWSCC mitigation, it appears necessary to discuss a more fundamental mechanistic experiment. Alloy 600 obtained from a vessel head penetration containing 16.05% chromium and Alloy 690 obtained from a steam generator tube plug containing 29.14% chromium were tested in simulated PWR primary water (1200 ppm B and 2 ppm Li) at 680 °F (360 °C) under electrochemical conditions corresponding to Ni/NiO equilibrium potential that corresponds to the maximum susceptibility of Alloy 600 to the initiation of PWSCC [8]. The resulting oxidized structures (corrosion scale and underlying metal) were examined by transmission electron microscopy (TEM) using cross section specimens. The oxide on Alloy 600 consisted of small 50 nm Ni(Cr,Fe)<sub>2</sub>O<sub>4</sub> and large 200 nm NiFe<sub>2</sub>O<sub>4</sub> crystallite oxides, while the oxide on Alloy 690 consisted of small 30 nm Ni(Cr,Fe)<sub>2</sub>O<sub>4</sub>

and large 100 nm  $\text{NiFe}_2\text{O}_4$  crystallite oxides, Figure 1-2. Alloy 690's oxide film was 50% thinner than Alloy 600's oxide film, which is characteristic of a more rupture resistant and protective oxide film.

For both alloys energy dispersive X-ray spectroscopy (EDX) analysis revealed chromium rich oxide layer where the underlying metal was chromium depleted, Figure 1-3. In both alloys a non-compact external oxide scale was identified while an inner thin continuous layer rich in chromium was observed. Consequently, a chromium depleted zone just in the underlying alloy was observed, Figure 1-4. For Alloy 600, the particular importance of the depletion was found to be also associated with the presence of oxygen. Chromium oxide was even found in a triple grain boundary as far as 3  $\mu\text{m}$  from the metal-oxide interface as sketched in Figure 1-5.

These test results tend to support the crack initiation mechanism induced by intergranular oxidation of the chromium depleted zones [9]. Assuming that this mechanism is operative in these exposure conditions, it is then possible to explain, at least in terms of local reactivity, the effect of the carbide precipitation sites (transgranular- intergranular) on the crack initiation resistance of Alloy 600 exposed to PWR experimental conditions. Most importantly for this evaluation, when considering Alloy 690, despite its chromium depletion from 29% to 17% in the underlying alloy, the chromium content of Alloy 690 remains is sufficiently high that the proposed intergranular oxidation mechanism becomes inoperative because the chromium content is greater than the 10% chromium needed to mitigate intergranular oxidation [10]. Thus, the apparent immunity of Alloy 690 to PWSCC can be explained. In contrast, Alloy 600 suffers PWSCC because its chromium content is also reduced by approximately 11 to 12% from only 16% down to 5%, which is below the 10% chromium "threshold" where internal oxidation occurs [1-8].

### 1.3 Discussion

The oxide mechanistic study results suggest that a chromium depletion of 11 to 12% occurs in nickel-base wrought alloys exposed to PWR environments under environmental conditions that clearly support and promote PWSCC. Since the internal oxidation "threshold" for these alloys is

approximately 10% chromium, then an additional 11 to 12% chromium should be initially present in the alloy to allow PWSCC mitigation. This suggests that an initial concentration of 21 to 22% chromium should be sufficient for PWSCC mitigation. This “threshold” value is consistent with the U-bend test results that indicated weld metals with between 22 and 30% chromium were very resistant to PWSCC. The results from the above Alloy 82 studies clearly suggest that 18 to 20% chromium is not sufficient to mitigate cracking. However, since Alloy 82, which can contain up to a specification limit of 22% chromium, does suffer PWSCC [1], the required chromium content to mitigate cracking must exceed 22%.

#### **1.4 Conclusion**

Albeit hampered by the paucity and fragmentary nature of the available effects of chromium on PWSCC data, the relevant available test data plus a mechanistic analysis suggests that the “threshold” chromium content for PWSCC mitigation is clearly >22% chromium. To provide some PWSCC margin, it is recommended that a 24% chromium content be the recommended compositional target for weld deposits to assure PWSCC protection.

Table 1-1  
Compositions of Nickel-base Alloys and Weld Metals

Alloying Element	Alloy 690 (Nuclear) [2]	Alloy 52 filler metal [3]	Alloy 152 electrode [3]	Alloy 72 filler metal (nominal) [4]	Alloy 600 [5]	Alloy 82 filler metal [3]	Alloy 182 electrode [3]	Alloy 132 electrode [1-3]
Ni + Co	58.0 min.	Balance	Balance	55	72.0 min.	67.0 min.	59.0 min.	62.0 min
C	0.04 max.	0.04 max.	0.05 max.	0.05	0.15 max.	0.10 max.	0.10 max.	0.08 max
Mn	0.5 max.	1.0 max.	5.0 max.	0.1	1.00 max.	2.5-3.5	5.0-9.5	3.5 max
Fe	7.0-11.0	7.0-11.0	7.0-12.0	0.2	6.00-11.00	3.0 max.	10.0 max.	11.0 max
S	0.015 max.	0.015 max.	0.015 max.	0.008	0.015 max.	0.015 max.	0.015 max.	0.02 max
Si	0.50 max.	0.50 max.	0.75 max.	0.1	0.50 max.	0.50 max.	1.0 max.	0.75 max
Mo		0.50 max.	0.50 max.					
Cu	0.50 max.	0.30 max.	0.50 max.	0.20	0.50 max.	0.50 max.	0.50 max.	0.50 max
Cr	28.0-31.0	28.0-31.5	28.0-31.5	44.0	14.0-17.0	18.0-22.0	13.0-17.0	13.0-17.0
Ti		1.0 max.	0.50 max.	0.6		0.75 max.	1.0 max.	
Al		1.10 max.	0.50 max.					
P		0.020 max.	0.030 max.			0.030 max.	0.030 max.	0.03 max
Nb + Ta		0.10 max.	1.0-2.5			2.0-3.0	1.0-2.5	1.5-4.0
Al + Ti		1.5 max.						
Others		0.50 max.	0.50 max.			0.50 max.	0.50 max.	0.50 max

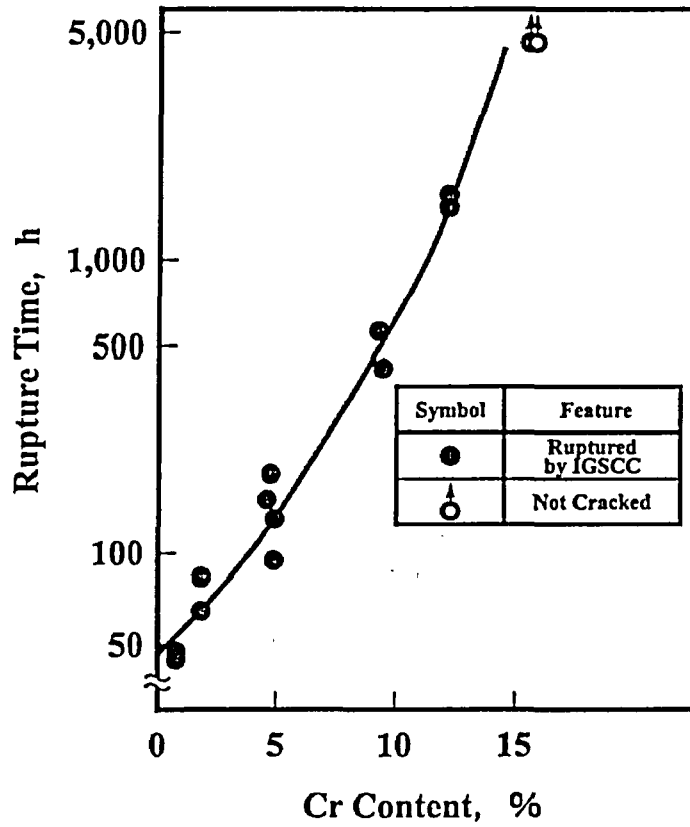


Figure 1-1. Effect of Chromium Content on the Stress Corrosion Cracking Resistance of Solution Annealed Ni-Cr-Fe Alloys [7]

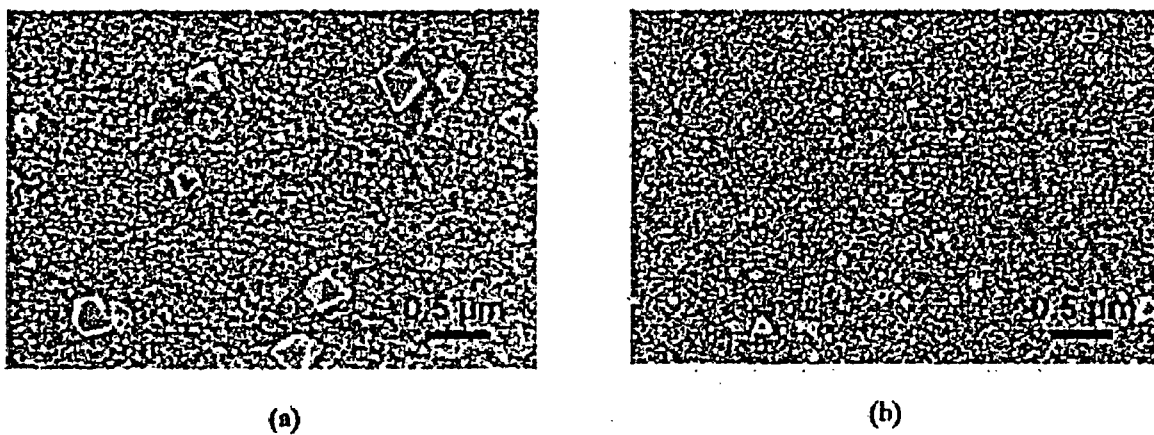
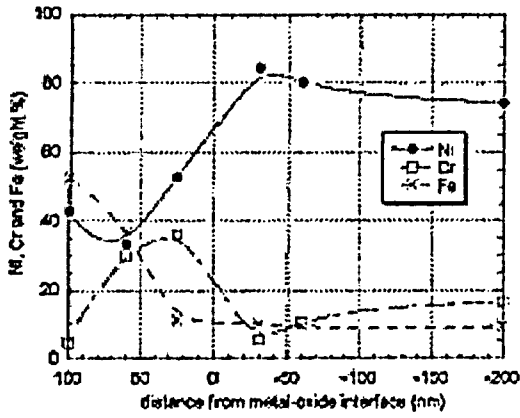
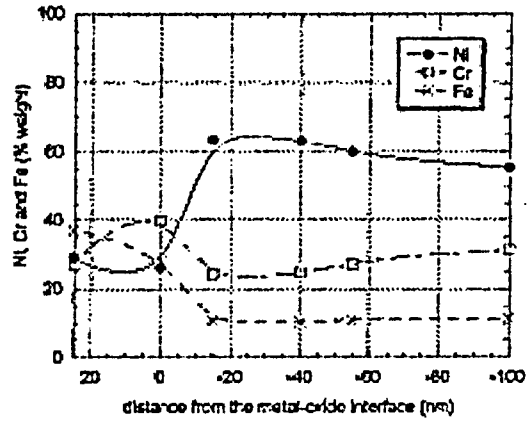


Figure 1-2. Oxide Film Developed on Alloy 600 (a) and Alloy 690 (b) [8]



(a)



(b)

Figure 1-3. Composition of Ni, Cr and Fe as a Function of the Distance from the Metal-Oxide Interface on Alloy 600 (a) and Alloy 690 (b). Note the difference in oxide thickness scale [8].

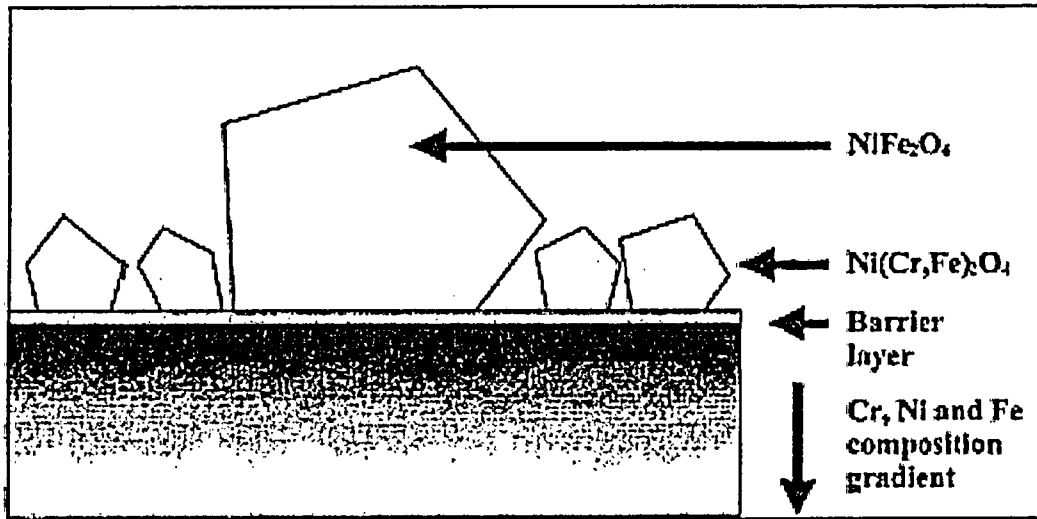


Figure 1-4. Sketch of the Oxide Film Developed on Alloy 600 and Consequences on the Underlying Metal [8]

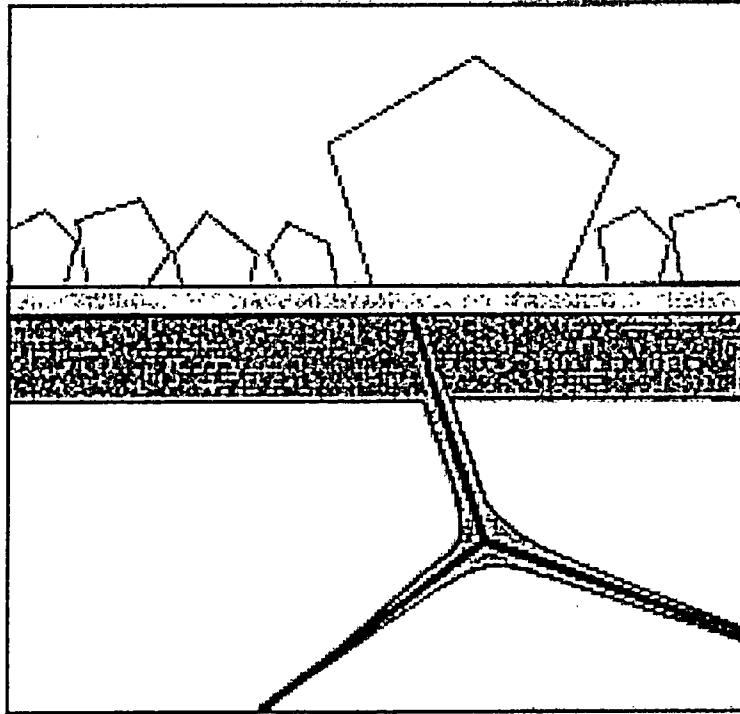


Figure 1-5. Sketch of the Depletion in Chromium under the Oxide Scale Associated with Enrichment in Oxygen at a Triple Grain Boundary [8]

## **2.0 CHROMIUM MEASUREMENT TECHNIQUE - X-RAY FLUORESCENCE**

### **2.1 Introduction**

Hand-held x-ray fluorescence (XRF) analyzers are able to quickly and non-destructively determine the “heavy” elemental composition of alloys [10]. More than 30 elements can be simultaneously quantified with great accuracy by measuring the characteristic fluorescence x-rays emitted by a target area. XRF analyzers quantify elements ranging from sulfur (element number 16) through uranium (element number 92) to the heaviest transuranic elements. In certain specialized laboratory applications, analyzers can also measure elements as light as aluminum and silicon (elements 13 and 14).

### **2.2 Background**

Each element in a specimen produces a unique set of characteristic x-rays that is a unique “fingerprint” for that specific element. XRF analyzers determine the chemistry of a sample by measuring the spectrum of the characteristic x-rays emitted by the compositional elements in the specimen when it is illuminated by high energy photons (e.g., x-rays or gamma rays). A fluorescent x-ray is created when a photon of sufficient energy strikes an atom in the sample, dislodging an electron from one of the atom’s inner orbital shells (lower quantum energy states), Figure 2-1. The atom subsequently regains stability, filling the vacancy left in the inner orbital shell with an electron from one of the atom’s higher quantum energy orbital shells. The electron drops to the lower energy state by releasing a fluorescent x-ray and the energy of this fluorescent x-ray (typically measured in electron volts, eV) is equal to the specific difference in energy between two quantum states of the dropping electron, Figure 2-2.

Because the quantum states of each electron orbital shell in each atom are different, the energies of the fluorescent x-rays produced by different elements are also different, i.e., each element present in the sample emits its own unique fluorescent x-ray energy spectrum. By inducing and measuring a wide spectrum of the range of different characteristic fluorescent x-rays emitted by the different elements in the sample, hand-held XRF analyzers can rapidly determine the

composition of the sample. For samples with known ranges of chemical composition, (e.g., Alloys 152, 52 and 690), analyzers can also identify many sample types by name, typically in seconds.

### 2.3 Sample Analysis Techniques

Although portable (< 2 lbs) XRF analyzers have inherent limitations in their ability to measure light elements, which is not a concern for the alloys presently under discussion, XRF analyzers automatically compensate for many other effects that would otherwise bias or distort sample analyses. These effects include:

- Geometric effects caused by the sample's shape, surface texture, thickness and density
- Spectroscopic interferences and other sample matrix effects
- Critical absorption of the characteristic x-rays of one element by other elements in the sample and secondary and tertiary x-ray excitation of one or more elements by other elements in the sample.

By automatically adjusting for these effects, XRF analyzers are able to determine the chemistries of samples of widely different sample compositions in typically in a few seconds, without any requirement for instrument users to input empirical, sample specific calibrations.

In typical samples containing many elements, the elements may range in concentrations from high percent levels down to parts per million (ppm). In sample matrices such as metal alloys, it is necessary to measure both lighter elements that emit lower energy x-rays that are easily absorbed as well as heavier elements that emit much higher energy x-rays.

### 2.4 Methodology

In the first empirical testing mode used in an XRF analyzers, Figure 2-3, the instrument user "teaches" a sample to the instrument with a one-minute measurement. The sample is named by the user and the sample's x-ray spectrum is stored in a dedicated library in the analyzer that can

hold hundreds of these spectra. When an unknown sample is measured in this mode, the new spectrum is compared to the taught spectra stored in the library via least-squares fit analyses. If the new sample location spectrum meets the specific sample-matching criteria (e.g. 24% Cr) for one of the stored sample spectra, the new sample is matched and identified by the given name of that stored sample. This signature-match mode is similar conceptually to doing fingerprint analysis.

In a second empirical testing mode, the instrument operator again “teaches” a sample area x-ray spectra to the analyzer and names the sample; then the user directly inputs a known (e.g. lab certified) chemical composition of the sample into the instrument. The sample area’s name, spectrum and chemistry are stored in a separate dedicated library. When an unknown sample area is measured in this mode, the sample area spectrum is compared to the sample spectra stored in this library. In this mode, the unknown sample area chemistry is calculated via extrapolation and interpolation from the stored chemistries of the named samples in the library and the calculated chemistry is then compared to a stored grade look-up table of chemical compositions. Empirical testing modes are especially well suited for measuring samples for which the chemical compositions are reasonably well known in advance, which will be the case for nickel-base weld metals.

## 2.5 Analytical Aspects

The two critical factors for the application of XRF analyzers are precision and accuracy. Precision is defined as the reproducibility of repeat measurements and can be quantified by the standard deviation. Accuracy is the relationship of the measured and actual value.

Some XRF analyzer precision data is presented in Table 2-1 for alloys similar to those of interest in this evaluation [12]. The standard deviations noted were calculated based on 11 field measurements for 20 seconds each. It should be noted that the precision shown in Table 2-1 is as good as laboratory measurements.

Correlation plots for two major alloy elements of interest (e.g., Cr and Mo) in iron, nickel and cobalt alloys as measured by X-ray tube excitation are presented in Figure 2-4 for 30 different alloys. The excellent agreement between certified and measured values is obvious even though the measurements were made in a single “alloy” mode or calibration mode in approximately one second.

Table 2-1

Examples of Precision of XRF Analyzer Measurements [12]

Alloy	Measurement	%Cr	%Mo	%Fe	%Ni	%W	%Mn
C-276	Mean	15.67	15.03	6.78	55.61	4.29	
	Std. Dev.	0.271	0.178	0.140	0.311	0.147	
	%RSD	1.73	1.16	2.06	0.56	3.43	
Type 316	Mean	17.21	2.38	67.99	10.17		1.76
	Std. Dev.	0.177	0.026	0.402	0.264		0.113
	%RSD	1.03	1.09	0.59	2.60		6.46

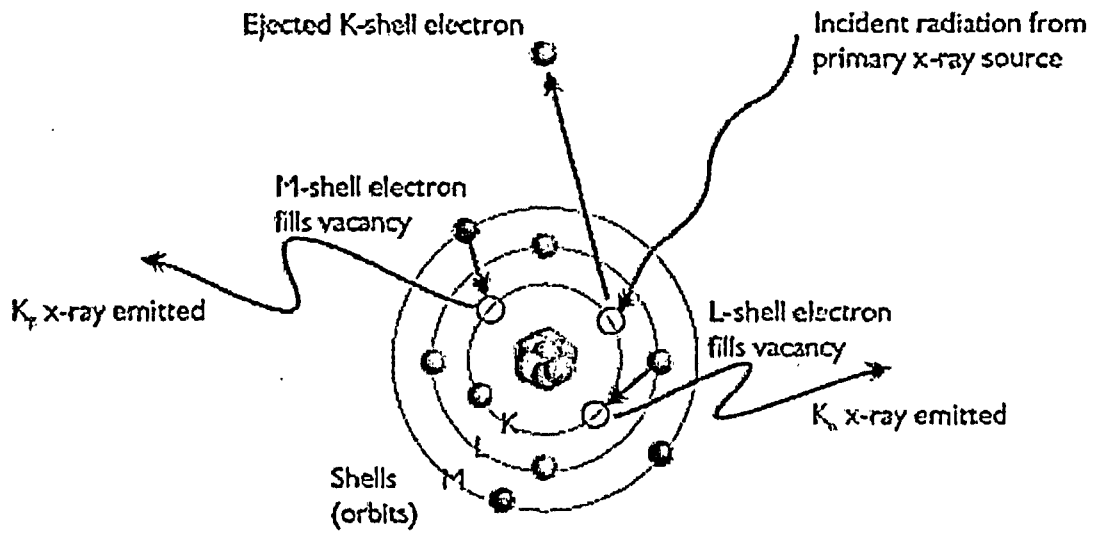


Figure 2-1. XRF Excitation Model [11]

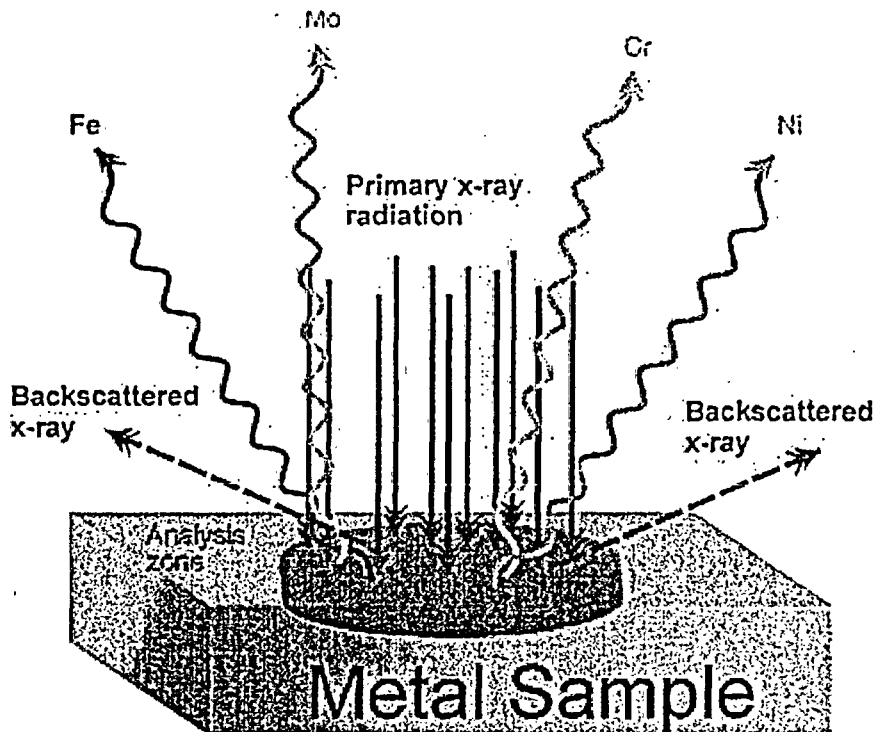
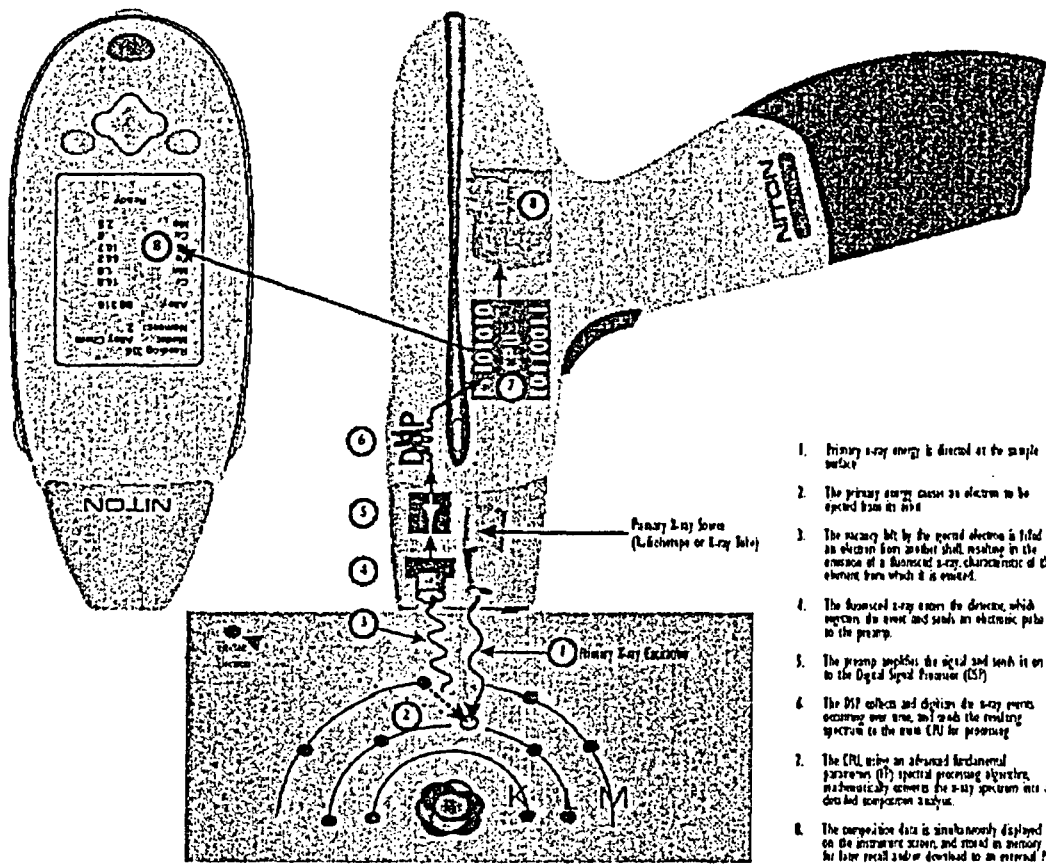


Figure 2-2. Metal Sample Fluorescence [11]



1. Primary x-ray energy is directed at the sample surface.
2. The primary energy causes an electron to be ejected from the shell.
3. The vacancy left by the ejected electron is filled by an electron from an outer shell, resulting in the emission of a fluorescent x-ray characteristic of the element from which it is emitted.
4. The fluorescent x-ray enters the detector, which registers the event and sends an electronic pulse to the processor.
5. The processor amplifies the signal and sends it on to the Digital Signal Processor (DSP).
6. The DSP collects and displays the x-ray events occurring over time, and sends the resulting spectrum to the main CPU for processing.
7. The CPU uses an advanced mathematical program (M) spectral processing algorithm, mathematically converts the x-ray spectrum into a detailed composition analysis.
8. The composition data is simultaneously displayed on the instrument screen, and stored in memory for later recall and/or download to an external PC.

Figure 2-3. Schematic of XRF Instrument [11]

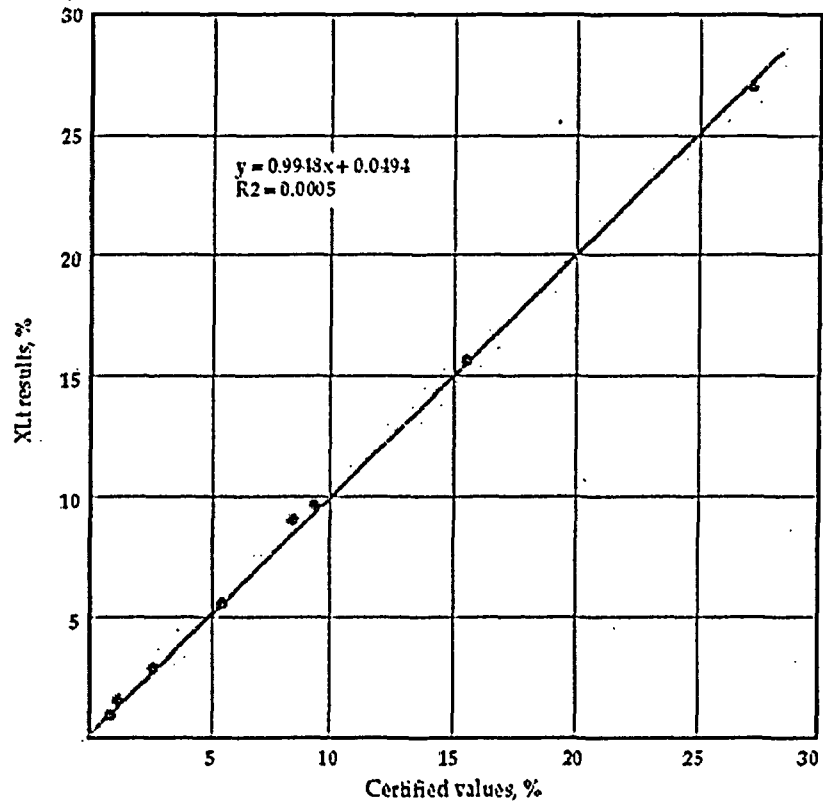


Figure 2-4. Correlation Plot for Cr and Mo in Various Fe, Co and Ni Alloys [12]

### **3.0 CHROMIUM CONTENT MEASUREMENT LOCATIONS**

#### **3.1 Introduction**

Now that the minimum chromium content has been recommended at 24% and the technique has been identified to accurately measure the chromium content, it is critical to also identify locations where chromium contents should be measured. It must be emphasized that the surface measurement of any Alloy 52 or 152 weld overlay for chromium content will be the maximum value, i.e., there will be a gradient of chromium content through the weld overlay where the maximum chromium dilution will occur at the interface between the substrate and the weld overlay. However, once the "recommended threshold" chromium value of 24% is met on the surface, PWSCC should not be able to propagate beyond that layer.

#### **3.2 Measurement Locations**

The selection of chromium measurement locations of an Alloy 152 or 52 weld overlay must obviously consider the substrate beneath the weld overlay. For example, a high-chromium (28.0-31.5% Cr) weld overlay will experience the greatest amount of alloy content dilution over a low alloy steel substrate. However, since low alloy steel is not susceptible to PWSCC, the weld overlay developed above the low alloy steel is used only for transferring the load across the defected weld or weld butter. Although the dilution of the Alloy 52 or 152 with the low alloy steel may produce an alloy with a chromium level below the recommended 24% level, there is no readily available path for PWSCC to propagate and, therefore, cracking through this layer is considered extremely unlikely.

A high-chromium weld overlay over Alloys 600, 182 and/or 82 will experience dramatically milder amounts of chromium dilution compared to the low alloy steel since these alloys chromium contents are dramatically higher at 14.0-17.0, 13.0-17.0 and 18.0-22.0 weight percent, respectively. Therefore, it appears that first priority location for the most conservative XRF measurement would be a location where Alloy 182 weld metal contacts a low alloy steel component, i.e., a butter, where the Alloy 182 is diluted by the low alloy steel and the high-

chromium weld overlay would be diluted by both materials, Figure 3-1. The next priority location would be where the higher chromium Alloy 82 is diluted by the low alloy steel. Using the same logic, Table 3-1 outlines an XRF priority inspection ranking for other interfaces and alloys based on simple chromium composition averages.

It should be noted that prioritizing the chromium measurement location along the length of the weld overlay is important. A measurement that shows the minimum chromium content has been realized at a high priority location should define a successful application without lots of additional measurements or resulting questions regarding what the chromium level is elsewhere along the length.

An acceptable chromium XRF measurement obtained from the first bead is the desired goal for PWSCC mitigation because it is this layer that could contact the environment. Therefore, XRF measurements should be made on the first pass. If the chromium content goal is indeed achieved, then the PWSCC mitigation requirement of the weld overlay would also be achieved. However, subsequent additional passes may be required to achieve the structural requirements. Measured chromium contents below 24% would necessitate additional weld overlay deposits.

Table 3-1  
XRF Measurement Locations Priorities

Substrate	Respective Cr Content Range	Estimated Interfacial Cr Content <sup>1</sup>	XRF Measurement Priority
low alloy steel/Alloy 182	1-3%/13-17	8	1
low alloy steel/Alloy 82	1-3%/18-22	10.5	2
Alloy 600/Alloy 182	14-17/13-17	15.25	3
Alloy 600	14-17	15.5	4
Type 304 stainless steel/Alloy 182	18-20/13-17	17	5
Alloy 600/Alloy 82	14-17/18-22	17.75	6
Type 304 stainless steel/Alloy 82	18-20/18-22	19.5	7

<sup>1</sup> Average of the mean of the range for each material in the pair

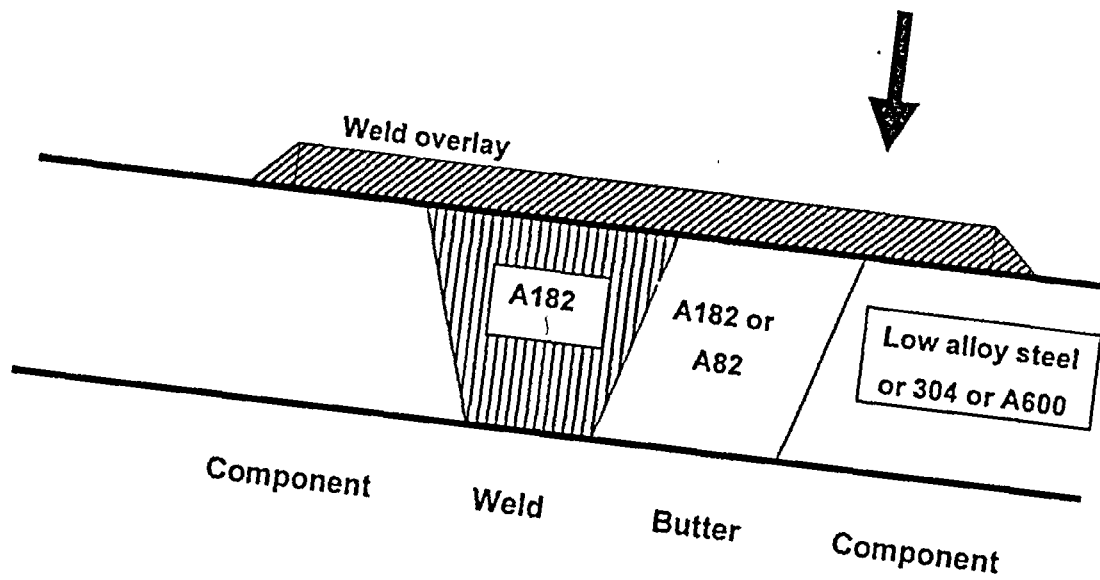


Figure 3-1. Sketch of XRF Inspection Locations

#### 4.0 REFERENCES

1. "Materials Reliability Program: Crack Growth Rates for Evaluating Primary Water Stress Corrosion Cracking of Alloy 82, 182, and 132 Welds (MRP-115)," EPRI, Palo Alto, CA: 2004. 1006696.
2. Special Metals Corporation, SMC-079, October 3, 2003.
3. Inco Alloy International, IAI-27-3/7M, 1993.
4. S. Kiser fax to B. M. Gordon, "Inconel Filler metal 72," May 2, 2000.
5. Special Metals Corporation, SMC-027, September 2, 2002.
6. D. Buisine, et al., "PWSCC Resistance of Nickel Based Weld Metals with Various Chromium Contents," Proceedings: 1994 EPRI Workshop on PWSCC of Alloy 600 in PWRs, EPRI, Palo Alto, CA: 1995. TR-105406, Paper D5.
7. T. Yonezawa, N. Sasaguri, and K. Onimura, "Effects of Metallurgical Factors on Stress Corrosion Cracking of Ni-base Alloys in High Temperature Water," Proceedings of the 1988 JAIF International Conference on Water Chemistry in Nuclear Power Plants, 1988, pp. 490–495.
8. J. Panter, et al., "Surface Layers on Alloys 600 and 690 in PWR Primary Water: Possible Influence on Stress Corrosion Crack Initiation," paper 02519 presented at Corrosion 2002, Houston, TX, April 7-11, 2002, NACE, Houston, TX.
9. P. M. Scott, "An Overview of Internal Oxidation as a Possible Explanation of Intergranular Stress Corrosion Cracking of Alloy 600 in PWRs," paper presented at the 9<sup>th</sup> International Symposium on Environmental Degradation of Materials in Nuclear Power Systems – Water Reactors, Newport Beach, CA, August 1-5, 1999, published in proceedings of same, TMS, Warrendale, PA, p. 387.
10. C. S. Giggins and F. S. Petit, "Oxidation of Ni-Cr Alloys between 800 and 1200 °C, Transaction of the Metallurgical Society of AIME, 245, 1969.
11. NITON Corporation, "NITON Sample Analysis Via Energy Dispersive X-Ray Fluorescence (EDXRF)," 2004.
12. V. B. E. Thomsen and D. Schatzlein, "X-Ray Fluorescence Spectrometry, Advanced Materials and Processes, August 2002.